International Journal for Multidisciplinary Research (IJFMR)
E-ISSN: 2582-2160 ● Website: www.ijfmr.com ● Email: editor@ijfmr.com

Development, Optimization, Characterization and Evaluation of Ibrutinib-Loaded Chitosan-Shelled Nanobubbles for Ultrasound-Responsive Targeted Drug Delivery

Ponnaganti Murali[1], Dr. Rakesh Kumar Meel[2], Dr. Narendra Kumar Nyola [3]

[1]Research Scholar
[2,3]Shridhar University, Pilani 333031

ABSTRACT

The present study focused on the development of nanosized Ibrutinib-loaded nanobubbles using a chitosan-based shell system. A 3^3 Box–Behnken Design (BBD) was employed to investigate the influence of three formulation variables, namely L-α-phosphatidylcholine (A), chitosan concentration (B), and palmitic acid concentration (C), on the particle size and polydispersity index (PDI) of the prepared nanobubbles. A total of 17 experimental runs were generated randomly using Design Expert® software, and the obtained data were evaluated through multiple regression analysis. Numerical optimization was applied to identify the optimum formulation by setting suitable constraints for the response variables.

Three optimized formulations (B1–B3) were selected and further characterized. Morphological analysis confirmed the formation of well-defined core–shell nanobubbles with particle sizes ranging between 150 and 200 nm. The optimized nanobubbles demonstrated an encapsulation efficiency of 82.58% and a drug loading capacity of 17% for Ibrutinib.

In vitro drug release studies showed that the optimized nanobubble formulation released 93.52% of Ibrutinib within 24 hours, which was considerably higher than the release observed from the conventional Ibrutinib suspension. Cellular uptake studies using HepG2 cells revealed enhanced fluorescence, with a mean fluorescence intensity of 6.12, approximately 1.5-fold greater than that obtained with Ibrutinib-loaded nanobubbles in the absence of ultrasound exposure. Furthermore, in vitro cytotoxicity results indicated that ultrasound-assisted nanobubbles promoted efficient intracellular drug release and improved therapeutic sensitivity.

Overall, the findings suggest that chitosan-shelled Ibrutinib nanobubbles represent a promising platform for contrast-enhanced tumor imaging as well as targeted therapeutic drug delivery.

Keywords: Ibrutinib, B-cell cancer, chitosan-shelled nanobubbles, perfluoropentane, Box–Behnken Design (BBD).

INTRODUCTION

Cancer-targeted nanotechnology has advanced rapidly over the past few decades, leading to the development of a wide range of nanoparticle-based drug delivery systems for cancer therapy [1]. Despite significant progress in nanomedicine research, only a limited number of these systems have successfully reached clinical application. For effective therapeutic action, drug-loaded nanocarriers must overcome several biological barriers following intravenous administration, selectively accumulate at the target site, and achieve efficient intracellular delivery. To address these challenges, researchers have investigated various controlled drug delivery strategies using nanocarriers. The therapeutic performance of these systems can be further enhanced through the application of external physical stimuli, such as electric, electromagnetic, or mechanical forces [2].

Among stimulus-responsive drug delivery systems, ultrasound (US)-triggered liposomes, micelles, and nanobubbles have emerged as promising platforms for site-specific drug release outside the bloodstream. Nanobubbles are nanosized spherical core–shell structures containing gases such as perfluorocarbons. They are specifically designed to improve stability, prolong circulation time, and enhance drug accumulation at the target tissue. Typically, their core is surrounded by a stabilizing shell composed of lipids, polymers, or albumin, which contributes to their structural integrity and drug delivery performance [3].

Chitosan-based nanobubbles have attracted considerable interest because of the unique properties of chitosan, including its natural origin, biodegradability, biocompatibility, low immunogenicity, and inherent antibacterial activity. Chitosan, a partially N-deacetylated derivative of chitin, is one of the most abundant naturally occurring polysaccharides. In addition to its excellent carrier properties, chitosan exhibits both direct and indirect antitumor activities, making it an attractive material for the delivery of anticancer agents [4].

Ibrutinib is a small-molecule inhibitor that irreversibly binds to Bruton's tyrosine kinase (BTK), thereby suppressing B-cell proliferation and survival. Inhibition of BTK blocks the B-cell receptor signaling pathway, which is frequently dysregulated in B-cell malignancies. Therefore, efficient delivery of ibrutinib has the potential to improve therapeutic outcomes in the treatment of B-cell cancers. In the present study, ibrutinib-loaded chitosan nanobubbles were developed with optimized particle size and physicochemical characteristics to enhance drug delivery efficiency and therapeutic efficacy.

Experimental design approaches have become valuable tools in pharmaceutical formulation development, as they minimize the number of experimental trials while providing comprehensive information regarding the influence of formulation variables. Statistical design of experiments (DoE) enables systematic evaluation of the relationship between independent variables and critical quality attributes of a formulation. Among these approaches, Response Surface Methodology (RSM) is widely employed for optimizing pharmaceutical formulations because it effectively evaluates both the individual and interactive effects of formulation variables. The Box–Behnken Design (BBD), a commonly used RSM approach, was selected in this study because it requires fewer experimental runs than other three-factor response surface designs while avoiding extreme experimental conditions. Accordingly, the objective of this research was to investigate the individual and interaction effects of formulation variables and to optimize the composition of ibrutinib-loaded chitosan nanobubbles using the Box–Behnken Design.

Materials and Methods

Materials

Ibrutinib was kindly provided as a gift sample by Dr. Reddy's Laboratories, Hyderabad, India. Chitosan and all other analytical-grade excipients were procured from Sigma-Aldrich, India. Perfluoropentane (PFP) was purchased from Pharm Affiliates, Haryana, India. All chemicals and reagents were used as received without further purification.

Preparation of Chitosan-Shelled Nanobubbles

Chitosan-shelled nanobubbles were prepared using perfluoropentane (PFP) as the gaseous core and chitosan (molecular weight ~190 kDa; degree of deacetylation 75–85%) as the shell-forming polymer. The formulation was prepared according to a previously reported method with slight modifications [6].

Briefly, L-α-phosphatidylcholine and palmitic acid were dissolved in 3 mL of ethanol and subsequently added to 5 mL of perfluoropentane under continuous magnetic stirring at room temperature to obtain a primary pre-emulsion. The resulting pre-emulsion was then diluted with ultrapure water and homogenized using a high-shear homogenizer (T25 Digital ULTRA-TURRAX®, IKA, Germany) at 12,000 rpm for 5 minutes under ice-bath conditions to produce a stable nanoemulsion.

A chitosan solution (pH 5.0) was added dropwise to the nanoemulsion under gentle magnetic stirring to facilitate the formation of chitosan-coated nanobubbles. The prepared nanobubble dispersion was purified by ultrafiltration using a TCF2 ultrafiltration system (Millipore, USA) equipped with a membrane having a molecular weight cut-off (MWCO) of 100 kDa to remove unentrapped components and residual solvents.

Finally, Pluronic® F68 (0.01% v/v) was added as a stabilizing agent to improve the colloidal stability of the nanobubble formulation. The formulation was allowed to equilibrate by incubation for 30 minutes before further physicochemical characterization.

Preparation of Ibrutinib-Loaded Chitosan Nanobubbles

Ibrutinib-loaded chitosan nanobubbles were prepared using the same procedure employed for the preparation of blank chitosan nanobubbles with slight modifications. Briefly, 100 mg of ibrutinib was dissolved in a mixture of perfluoropentane and ethanol, where ethanol served as a co-solvent to facilitate uniform drug dispersion within the perfluoropentane core. L-α-phosphatidylcholine and palmitic acid were dissolved separately in ethanol and subsequently mixed with the drug-containing perfluoropentane solution under continuous magnetic stirring to obtain a homogeneous pre-emulsion.

The resulting pre-emulsion was diluted with ultrapure water and homogenized using a high-shear homogenizer under optimized conditions. Thereafter, the chitosan solution (pH 5.0) was added dropwise with gentle magnetic stirring to form the chitosan shell around the perfluoropentane core. The prepared nanobubbles were purified by ultrafiltration to remove unencapsulated drug and excess reagents, followed by the addition of Pluronic® F68 (0.01% v/v) as a stabilizing agent. The final formulation was incubated for 30 minutes before further characterization.

Optimization of Critical Formulation Parameters Using Design of Experiments

Based on preliminary investigations, the concentrations of L-α-phosphatidylcholine (Factor A), chitosan (Factor B), and palmitic acid (Factor C) were identified as the critical formulation variables influencing the particle size and polydispersity index (PDI) of the nanobubbles. Therefore, a three-factor, three-level Box–Behnken Design (BBD) was employed to systematically investigate the effects of these independent variables and to optimize the formulation.

The range and levels of each independent variable were selected based on the results of preliminary experiments and are summarized in **Table 1**. According to the BBD matrix, a total of 17 experimental runs were generated and randomized using Design-Expert® software to minimize experimental bias. The formulation composition and experimental conditions for all runs are presented in **Table 2**.

Statistical Analysis

The experimental data obtained from the Box–Behnken Design were analyzed using Design-Expert® software. The relationships between the independent variables and the measured responses were evaluated by fitting the data to appropriate mathematical models. Model selection was based on several statistical parameters, including the model *p*-value, lack-of-fit *p*-value, coefficient of determination (R^2), adjusted R^2, predicted R^2, and coefficient of variation (CV).

Terms with a *p*-value less than 0.05 were considered statistically significant and retained in the final model, whereas non-significant terms ($p > 0.05$) were excluded whenever appropriate to improve model predictability. The optimized response variables, including particle size and polydispersity index, were described using a second-order polynomial (quadratic) equation generated through multiple regression analysis, as represented in **Equation (1)**.

$$Y = A_0 + A_1X_1 + A_2X_2 + A_3X_3 + A_4X_1^2 + A_5X_2^2 + A_6X_3^2 + A_7X_1X_2 + A_8X_1X_3 + A_9X_2X_3 \quad (1)$$

Where,

Y	Response parameter
A_0	Intercept
$A_1 – A_9$	Regression coefficients
X_1, X_2 and X_3	Main influencing factors
X_1 X_2	Interactive effect
X_1^2, X_2^2 ,X_3^2	Quadratic effect

During model development, non-significant independent variables that did not meaningfully contribute to the regression equation were eliminated sequentially using the backward elimination method to obtain the most appropriate predictive model. The relationships between the independent variables and the response parameters were further evaluated using three-dimensional response surface plots (3D-RSPs), which illustrate the combined effects of two formulation variables on a selected response while maintaining the third variable at a constant level. In addition, perturbation plots and contour plots (CPs) were generated to visualize the individual and interactive effects of the formulation variables on the measured responses and to facilitate identification of the optimum design space.

Formulation Optimization

Numerical optimization was performed to determine the optimal levels of the independent formulation variables by applying predefined constraints to both the formulation factors and the response parameters. The optimized formulation was selected based on the desired criteria of minimum particle size and polydispersity index while satisfying all optimization constraints. To validate the optimization process, the optimized ibrutinib-loaded chitosan nanobubble formulation was prepared in triplicate under the

predicted optimum conditions, and the experimental results were compared with the values predicted by the optimization model to assess its accuracy and reliability.

Table 1: BBD

Factor			**Levels**		
Variable		Units	Low	Intermediate	High
A	Conc. of L-α-Phosphatidylcholine	w/v	1	1.5	2
B	Conc. of Chitosan	w/v	1	2	3
C	Conc. of palmitic acid	w/v	0.5	1	1.5
Responses			**Goal**		
Y1	PLS	nm	Decrease		
Y2	PI	-	Decrease		

Characterization of Nanobubble Formulation

Determination of Particle Size, Polydispersity Index, and Zeta Potential

The particle size (PS), polydispersity index (PDI), and zeta potential (ZP) of the prepared nanobubble formulations were determined using a Malvern particle size analyzer (Mastersizer 2000, Malvern Instruments, UK) based on the principle of dynamic light scattering (DLS) [7]. Prior to analysis, the formulations were appropriately diluted with ultrapure water.

The average particle size and PDI were determined by measuring the fluctuations in the intensity of scattered light caused by the Brownian motion of the nanobubbles. The zeta potential was measured using a gold-plated electrode fitted with a U-shaped electrophoretic cell to evaluate the surface charge and colloidal stability of the formulation. All measurements were performed at 25°C, and each sample was analyzed in triplicate. The results were expressed as mean ± standard deviation.

Transmission Electron Microscopy (TEM)

The morphology and structural characteristics of the prepared nanobubbles were examined using a transmission electron microscope (JEOL JEM-2000FX, JEOL Ltd., Japan) [8]. For TEM analysis, the formulation was suitably diluted with ultrapure water, and a drop of the diluted sample was placed on a carbon-coated copper grid. The sample was negatively stained with an aqueous phosphotungstic acid solution to enhance image contrast and allowed to air-dry before analysis. The stained samples were then observed under the transmission electron microscope to evaluate the morphology, size, and structural integrity of the nanobubbles.

Table 2: Observed responses of trial experiments as per BBD

Expt	**A (w/v)**	**B (w/v)**	**C (w/v)**	**PLS (nm)**	**PI**
1	1.5	2	1	398.23	0.26
2	1.5	3	1.5	198.12	0.16
3	1	1	1	322.72	0.32
4	1	2	0.5	416.42	0.51

5	1.5	2	1	394.16	0.27
6	1	3	1	246.72	0.29
7	2	3	1	252.78	0.28
8	1	2	1.5	345.72	0.2
9	2	2	1.5	368.34	0.26
10	2	1	1	326.18	0.32
11	1.5	2	1	400.12	0.27
12	1.5	3	0.5	272.46	0.44
13	1.5	1	1.5	293.12	0.22
14	1.5	2	1	399.12	0.25
15	2	2	0.5	402.82	0.44
16	1.5	1	0.5	322.42	0.43
17	1.5	2	1	396.44	0.26

Determination of Encapsulation Efficiency and Drug Loading Capacity

The encapsulation efficiency (EE) and drug loading capacity (DLC) of the ibrutinib-loaded chitosan nanobubbles were determined using the dialysis method [9]. Briefly, 5 mL of the nanobubble formulation (equivalent to approximately 1 mg of ibrutinib) was transferred into a dialysis bag (molecular weight cut-off: 12,000–14,000 Da) and immersed in 100 mL of phosphate buffer (pH 7.4) containing 1 M sodium thiocyanate as the dialysis medium.

The dialysis study was carried out at 37 ± 0.5°C under continuous magnetic stirring at 100 rpm. After 60 minutes, a 2 mL aliquot was withdrawn from the dialysis medium to determine the amount of unencapsulated (free) drug. The formulation remaining inside the dialysis bag was then disrupted by dissolving it in a mixture of water and methanol to extract the encapsulated drug completely.

The concentrations of both free and encapsulated ibrutinib were quantified using a validated stability-indicating high-performance liquid chromatography (HPLC) method. The percentage encapsulation efficiency (EE%) and drug loading capacity (DLC%) were calculated using the following equations:

$$Encapsulation\ efficiency = \frac{(Total\ amount\ of\ inbrutinib - Free\ ibrutinib)}{Total\ amount\ of\ ibrutinib}$$

$$Loading\ capacity = \frac{(Total\ amount\ of\ inbrutinib - Free\ ibrutinib)}{Weight\ of\ nanobubbles\ formulation}$$

Viscosity and Refractive Index

The viscosity and refractive index of the prepared nanobubble formulations were determined at 25°C using a capillary viscometer and an Abbe refractometer, respectively. All measurements were performed under ambient laboratory conditions, and the average values were recorded.

Differential Scanning Calorimetry (DSC)

The thermal behavior of the pure drug, excipients, and optimized nanobubble formulation was evaluated using a Differential Scanning Calorimeter (PerkinElmer STA 8000 Thermal Analyzer). Approximately 5

mg of each sample was accurately weighed into a sealed aluminum sample pan, while an empty aluminum pan was used as the reference. The samples were heated from 30°C to 400°C at a heating rate of 10°C/min under a continuous nitrogen atmosphere. Each sample was analyzed in triplicate to ensure reproducibility of the results.

In Vitro Drug Release Study

The in vitro release profile of ibrutinib from the chitosan nanobubbles was evaluated using the dialysis bag diffusion technique at 37 ± 0.5°C in phosphate buffer (pH 7.4), both in the presence and absence of ultrasound stimulation [10]. The nanobubble formulation was placed in a dialysis bag and immersed in the release medium under continuous stirring. At predetermined time intervals, 1 mL of the release medium was withdrawn and replaced with an equal volume of fresh phosphate buffer to maintain sink conditions.

Drug release was monitored for up to 24 hours. Ultrasound-triggered drug release was evaluated by exposing the formulation to ultrasound at a frequency of 2.5 ± 0.1 MHz for 1 minute prior to the release study. The collected samples were analyzed spectrophotometrically to determine the amount of ibrutinib released at each sampling interval.

Ultrasound Stability of Ibrutinib-Loaded Nanobubbles

The stability of the ibrutinib-loaded nanobubbles under ultrasound exposure was investigated by subjecting the formulation to an ultrasound stimulus with an oscillation frequency of 2.5 ± 0.2 MHz, an average acoustic pressure of 2.5 ± 0.2 MPa, a nominal frequency of 50 Hz, and a nominal power output of 30 W [11]. The formulations were exposed to ultrasound for different durations (30 seconds, 1, 2, 3, 4, and 5 minutes) at 37°C. After each exposure, the samples were allowed to stand for 10 minutes before examination. The morphology and structural integrity of the nanobubbles were assessed using optical microscopy and compared with the untreated formulation.

Stability Study of Ibrutinib-Loaded Nanobubbles

The physical stability of the optimized ibrutinib-loaded nanobubbles was evaluated by storing the formulations at 4°C, 25°C, and 40°C for a period of one month [11]. Samples were withdrawn on the 1st, 10th, and 30th day to determine drug content, encapsulation efficiency, and mean particle size. In addition, the appearance and structural integrity of the nanobubbles were examined using optical microscopy throughout the storage period to assess any changes in morphology or stability.

Determination of Hemolytic Activity

The hemocompatibility of the chitosan nanobubble formulation was evaluated by determining its hemolytic activity using human erythrocytes [12]. Nanobubble formulations at different concentrations (1%, 2%, 4%, 6%, 8%, and 10% v/v) were incubated with a 30% (v/v) erythrocyte suspension prepared in phosphate buffer (pH 7.4). A suspension of erythrocytes in phosphate buffer served as the negative control, while complete hemolysis was achieved by treating the erythrocytes with an excess of ammonium chloride, which served as the positive control.

The samples were incubated at 37°C for 2 hours and subsequently centrifuged at 3000 rpm for 10 minutes. The absorbance of the collected supernatants was measured spectrophotometrically at 543 nm.

The percentage hemolysis was calculated by comparing the absorbance of the test samples with that of the positive control (100% hemolysis) using the following equation.

$$\% \, Hemolysis = \frac{ABS_{Sample} - ABS_0}{ABS_{100} - ABS_0} + 100$$

Where ABS_0 and ABS_{100} are the absorbance of the solution at 0 and 100 % hemolysis, respectively

In Vitro Cellular Uptake Study

The cellular uptake of free ibrutinib and ibrutinib-loaded chitosan nanobubbles was qualitatively evaluated using confocal laser scanning microscopy (CLSM) [13]. HepG2 cells were seeded into confocal culture chambers and allowed to attach overnight under standard cell culture conditions. The cells were then treated with free ibrutinib dissolved in dimethyl sulfoxide (DMSO) (50 μM), ibrutinib-loaded nanobubbles without ultrasound exposure (50 μM), and ibrutinib-loaded nanobubbles following ultrasound treatment (50 μM).

At predetermined time intervals, the cells were washed with phosphate-buffered saline (PBS) and visualized using a confocal laser scanning microscope under blue fluorescence with an excitation wavelength of 405 nm. For quantitative fluorescence analysis, the treated cells were incubated for 2 hours, after which the fluorescence intensity was measured using a fluorescence microplate reader at excitation and emission wavelengths of 503 nm and 528 nm, respectively. All experiments were performed in triplicate, and the mean fluorescence intensity was used to assess the cellular uptake efficiency of the different formulations.

In Vitro Cytotoxicity Assay

The cytotoxicity of free ibrutinib and ibrutinib-loaded nanobubbles was evaluated using the MTT assay on HepG2 cells [14]. The cells were cultured in Dulbecco's Modified Eagle Medium (DMEM) supplemented with 10% fetal bovine serum (FBS) and maintained at 37°C in a humidified atmosphere containing 5% CO_2. HepG2 cells were seeded into 96-well plates at a density of 5×10^4 cells per well and incubated overnight to allow cell attachment.

Following incubation, the cells were treated with blank nanobubbles, free ibrutinib dissolved in DMSO, ibrutinib-loaded nanobubbles without ultrasound exposure (50 μM), and ibrutinib-loaded nanobubbles with ultrasound exposure (50 μM) at the desired concentrations. The ratio of culture medium to formulation was maintained at 9:1 in each well. After incubation for 24 and 48 hours, 20 μL of MTT solution (5 mg/mL) was added to each well, and the plates were further incubated for 4 hours. The culture medium was then carefully removed, and dimethyl sulfoxide (DMSO) was added to dissolve the formed formazan crystals. The absorbance of each well was measured at 570 nm using a microplate reader (Model 680, Bio-Rad Laboratories, Hercules, CA, USA). Cell viability was calculated by comparing the absorbance of treated cells with that of the untreated control group.

Statistical Analysis

All experimental data are presented as mean ± standard deviation (SD) of at least three independent experiments. Statistical analysis was performed using the unpaired Student's *t*-test. Differences were considered statistically significant at $p < 0.05$.

Results and Discussion

A total of seventeen experimental formulations were prepared according to the three-factor, three-level Box–Behnken Design (BBD). The experimental design matrix and the corresponding responses for the selected independent and dependent variables are presented in **Table 4**. Different batches of ibrutinib-loaded chitosan nanobubbles were formulated by varying the concentrations of L-α-phosphatidylcholine, chitosan, and palmitic acid. Preliminary investigations revealed considerable variations in particle size and polydispersity index among the prepared formulations, indicating that the composition of the formulation had a significant influence on the physicochemical characteristics of the nanobubbles.

Based on these preliminary observations, the concentrations of L-α-phosphatidylcholine (Factor A), chitosan (Factor B), and palmitic acid (Factor C) were selected as the critical formulation variables for optimization. The Box–Behnken Design was subsequently employed to evaluate the individual and interactive effects of these variables on particle size and polydispersity index. Statistical analysis demonstrated that the selected quadratic model was significant for both response variables, as indicated by model *p*-values less than 0.05. The experimental design and summary of the optimization process are presented in **Figure 1**.

Study Type	Response Surface	**Runs**	17
Design Type	Box-Behnken	**Blocks**	No Blocks
Design Model	Quadratic	**Build Time (ms)**	45.88

Factor	Name	Units	Type	Subtype	Min.	Max.	-1 Actual	+1 Actual	Mean	Std. Dev
A	Concentration of L-alpha	w/v	Numeric	Continuous	1.00	2.00	1.00	2.00	1.50	0.34
B	Concentration of chitosan	w/v	Numeric	Continuous	1.00	3.00	1.00	3.00	2.00	0.69
C	Concentration of palmitic acid	w/v	Numeric	Continuous	0.50	1.50	0.50	1.50	1.00	0.34

Response	Name	Units	Obs	Analysis	Min.	Max.	Mean	Std. Dev.	Ratio	Trans	Model
Y1	Particular size	Nm	17	Polynomial	198.12	416.42	338.617	66.7437	2.10186	None	RQuadratic
Y2	Ploydispersity index		17	Polynomial	0.16	0.51	0.304706	0.095598	3.1875	None	RQuadratic

Response Surface Methodology (RSM) Optimization

Statistical Analysis

The particle size (Y_1) of the prepared nanobubble formulations ranged from **198.12 to 416.42 nm**, whereas the polydispersity index (PDI, Y_2) varied between **0.16 and 0.51**. The experimental data obtained from all 17 formulations were fitted to various mathematical models, and a second-order

quadratic model was found to best describe the relationship between the independent formulation variables and the selected responses.

The suitability of the quadratic model was evaluated using analysis of variance (ANOVA), lack-of-fit analysis, and the coefficient of determination (R^2). The statistical analysis confirmed that the selected model was significant and adequately represented the experimental data, as evidenced by the significant model *p*-value, non-significant lack-of-fit, and high R^2 values. The statistical parameters used for model evaluation are summarized in **Table 3**.

Table 3: Regression equations for the responses

Dependent Variable	Regression equation
Y1	397.9784 + 2.3175 A – 36.795 B – 26.1025 C + 9.055 AC – 11.26 BC – 111.184 B^2 - 14.9589 C^2
Y2	0.262105-0.0025 A-0.015 B-0.1225 C + 0.0325 AC – 0.0175 BC + 0.040263 A^2 + 0.050263 C^2

Particle Size

The particle size (PS) of the prepared nanobubble formulations was found to be within the range of **198.12–416.42 nm** [15]. The polynomial model obtained from the response surface analysis demonstrated that all three independent variables, including the concentration of L-α-phosphatidylcholine (A), chitosan concentration (B), and palmitic acid concentration (C), had a significant influence on the particle size of the nanobubbles.

The response surface plots were used to evaluate the individual and interactive effects of the formulation variables on particle size. The combined effect of variables A and C while maintaining variable B at a constant level was analyzed using response surface plots, as presented in **Figures 2 and 3**. Similarly, the interaction between variables B and C at a fixed level of variable A was evaluated, and the corresponding response surface plots are shown in **Figures 4, 5, and 6**. These plots illustrate the influence of formulation composition and variable interactions on the particle size of the nanobubbles.

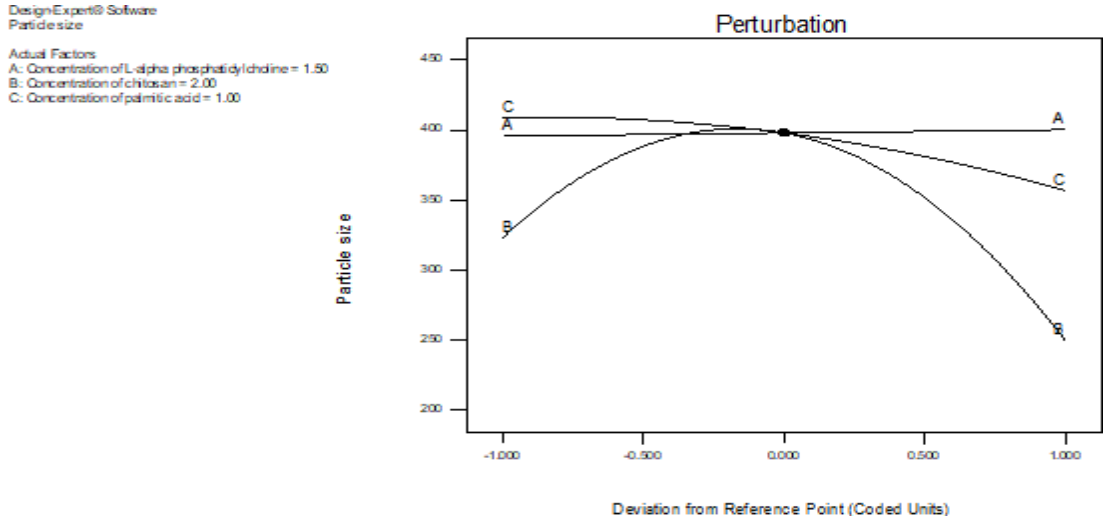

Figure 2: Two dimensional PP– impact of A, B and C on PLS

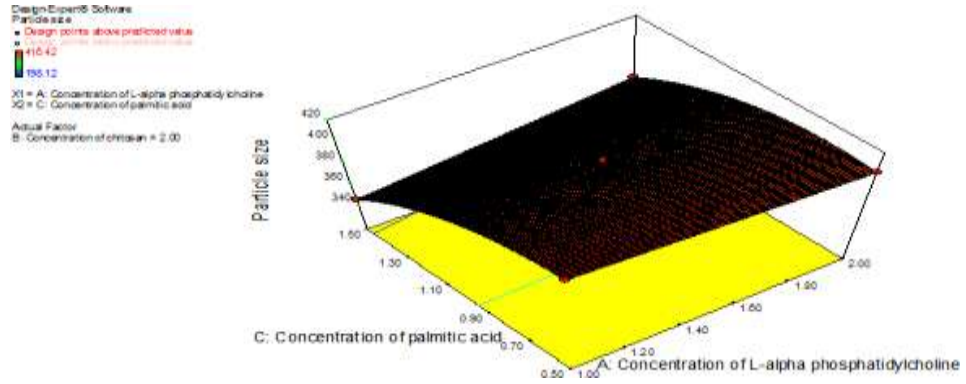

Figure 3: 3D- RSP showcasing the impact of A & C on PLS at constant level of B

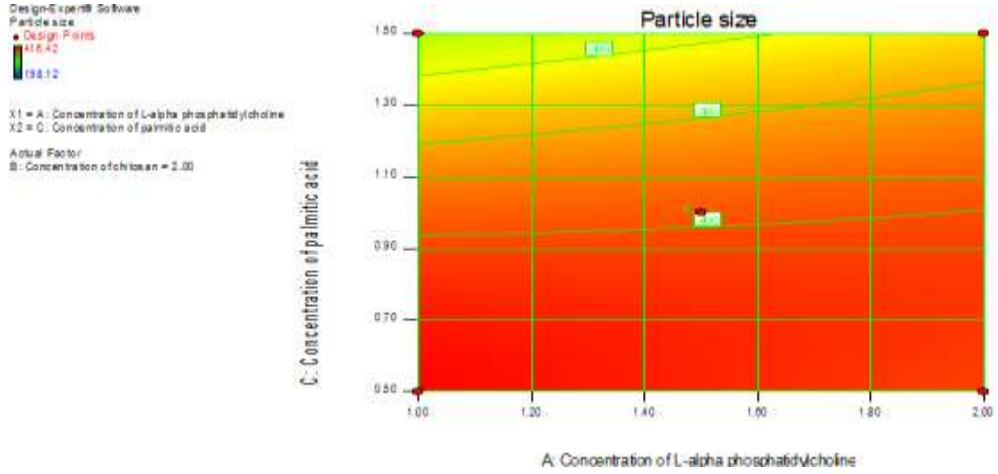

Figure 4: CP showcasing the impact of A and C on PLS at constant level of B

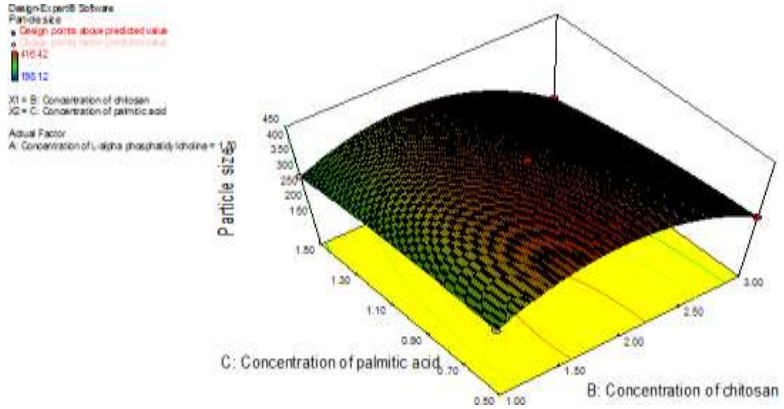

Figure 5:3D- RSP showcasing the impact of B & C on PLS at constant level of A

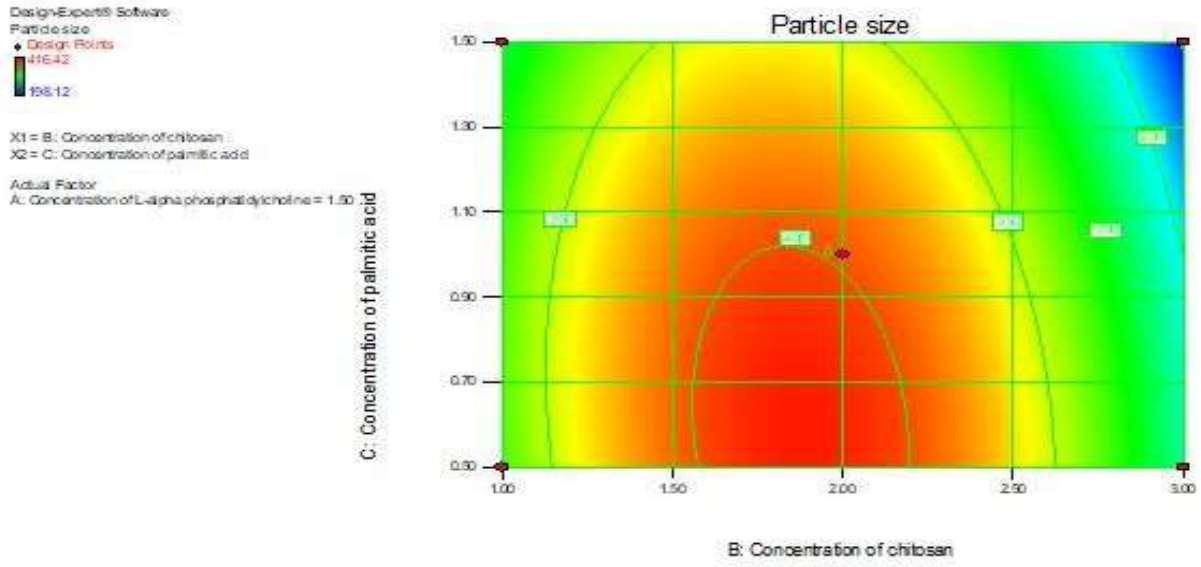

Figure 6: CP showcasing the impact of B & C on PLS at constant level of A

Polydispersity Index (PDI)

The polydispersity index (PDI) values of the prepared nanobubble formulations were observed to be within the range of **0.16–0.51**. The polynomial model obtained from the response surface analysis revealed that all the selected formulation variables (A, B, and C) had a significant effect on the PDI of the nanobubbles. The experimentally obtained values were found to be in close agreement with the predicted values generated by the model, indicating the reliability and accuracy of the developed formulation model.

The two-dimensional (2D) and three-dimensional (3D) response surface plots demonstrated the influence of individual and interactive effects of the formulation variables on PDI. Among the selected variables, factor C exhibited the most pronounced effect on PDI, followed by factor B, whereas factor A showed comparatively less influence. The interaction effect between variables A and C at a fixed level of variable B was evaluated using response surface plots, as shown in **Figures 7 and 8**. Similarly, the combined effect of variables B and C while maintaining variable A at a constant level was analyzed, and the corresponding plots are presented in **Figures 9, 10, and 11**. These results indicate that the concentration of formulation components plays an important role in controlling the uniformity and size distribution of the nanobubble system.

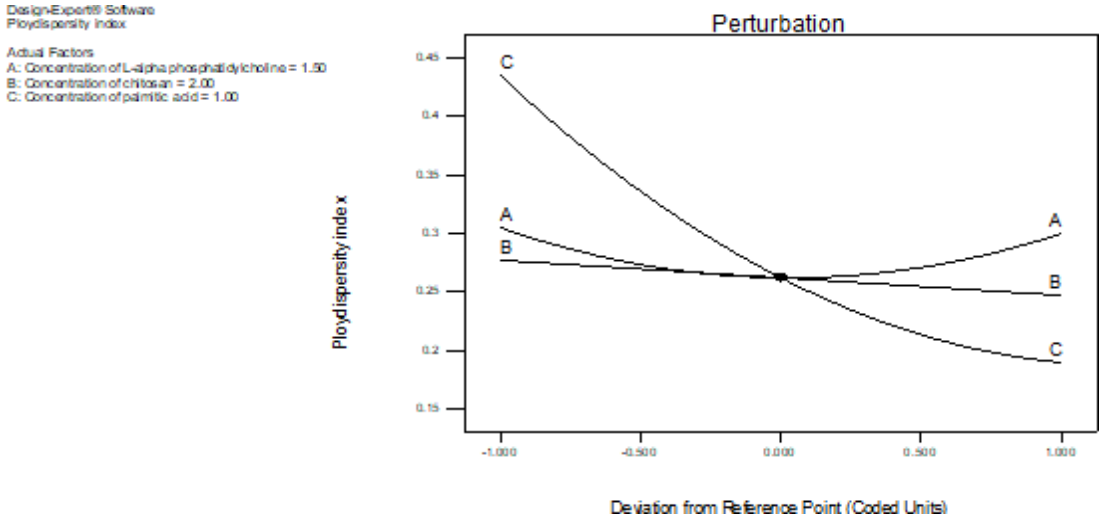

Figure 7: Two dimensional PP– impact of A, B & C on PI

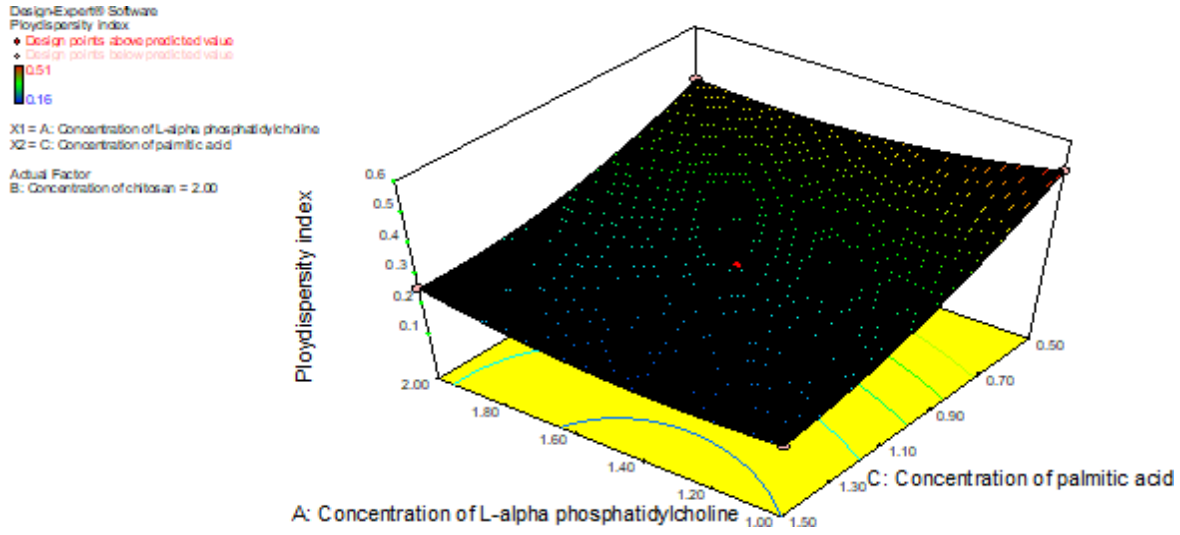

Figure 8: 3D- RSP showcasing the impact of A & C on PI at constant level of B

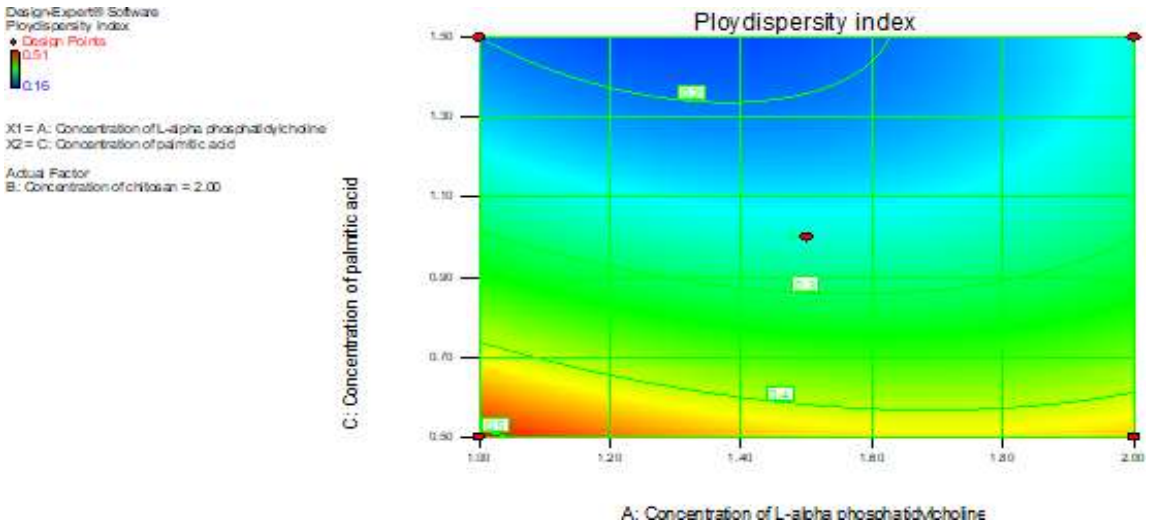

Figure 9: CP showcasing the interactive impact of A &C on PI at constant level of B

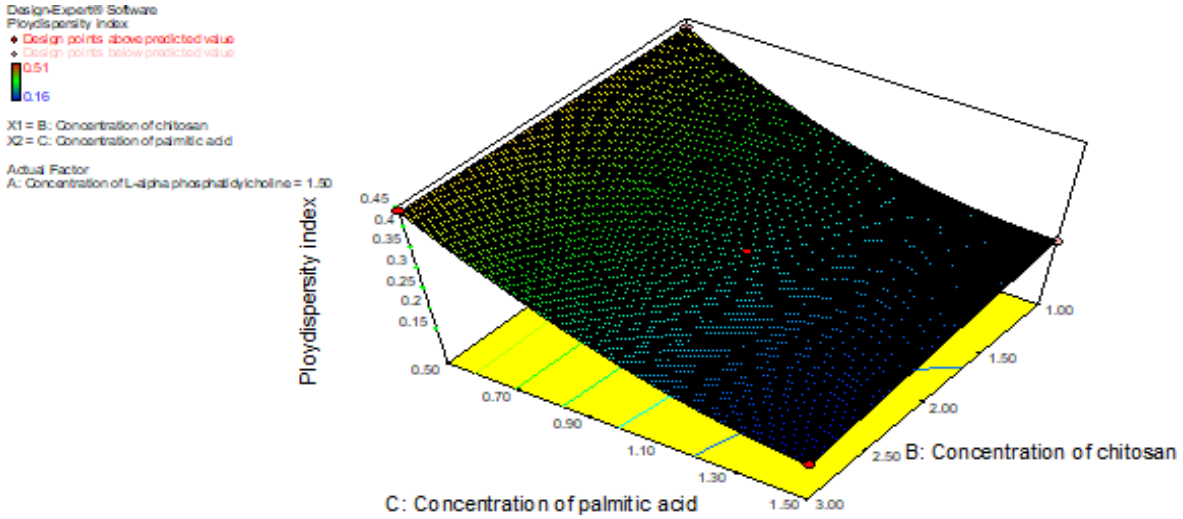

Figure 10:3D- RSP showcasing the impact of B & C on PI at constant level of A

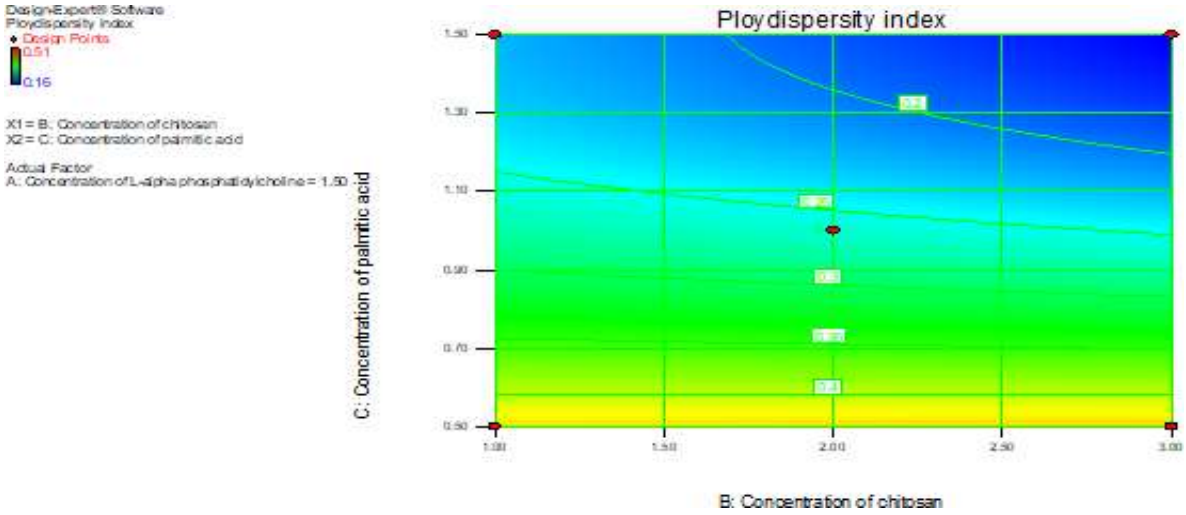

Figure 11: The CP showcasing the interactive impact of B & C on PI at constant level of A

Optimization

The optimization of formulation variables was performed using the Derringer's desirability function approach to identify the optimum conditions for achieving the desired response parameters. The selected responses, including particle size (PS) and polydispersity index (PDI), were transformed into individual desirability values, and the overall desirability function (D) was calculated by considering the maximum and minimum response limits as the optimization criteria.

The highest desirability value (**D = 0.993**) was obtained at the optimized formulation conditions of **1.11% w/v L-α-phosphatidylcholine (A), 2.95% w/v chitosan (B), and 1.5% w/v palmitic acid (C)**. To validate the optimization model, three independent batches of ibrutinib-loaded nanobubbles were prepared under the optimized conditions. The observed response values of these optimized batches are presented in **Table 4**.

A close correlation was observed between the predicted and experimental response values, confirming the reliability of the Box–Behnken Design (BBD) combined with the Derringer's desirability approach for the successful optimization of the ibrutinib-loaded nanobubble formulation.

The optimized ibrutinib-loaded nanobubble formulations exhibited comparable particle size values with low PDI, indicating a narrow and uniform particle size distribution. Transmission electron microscopy (TEM) analysis confirmed the spherical morphology and core–shell structure of the nanobubbles, with particle sizes observed in the range of **150–200 nm** (**Figure 12**). Furthermore, the particle size obtained from TEM analysis showed good agreement with the values determined by dynamic light scattering (DLS), confirming the accuracy of the particle size measurement.

Table 4: Optimum conditions attained by applying restrictions on response parameters

Independent variables	**Optimized values**	**Predicted values**		**Actual values**			
		PLS(Y1)nm	**PI (Y2)**	**Batch**	**PLS(Y1)nm**	**PI (Y2)**	**ZP(mV)**
Concentration of L-α-Phosphatidylcholine	1.11	201.329	0.15999	B1	198.36± 8.34	0.17± 0.005	38.34±3.36
Concentrationof Chitosan	2.95			B2	206.18± 6.28	0.18± 0.005	42.88±2.28
Concentrationof palmiticacid	1.5			B3	201.66± 7.12	0.16± 0.005	39.76±1.89

Table 5: Physical characteristics of nanobubbles

	Blank nanobubbles	**Ibrutinib loaded nanobubbles**
Average particle size	199.82±10.12	201.66±7.12
Polydispersity index	0.20± 0.005	0.16± 0.005
Zeta potential	52.36±2.42	39.76±1.89
Encapsulation efficiency	-	82.58±3.17
Loading capacity	-	17.12±2.66

The optimized nanobubble formulation demonstrated efficient incorporation of ibrutinib within the nanobubble structure, exhibiting an encapsulation efficiency of **82.58%** and a drug loading capacity of **17%** (**Table 5**). The high encapsulation efficiency indicates the effective entrapment of ibrutinib within the chitosan-shelled nanobubble system.

Furthermore, the incorporation of ibrutinib into the nanobubble formulation did not produce any significant alteration in the viscosity of the formulation, suggesting that drug loading had minimal influence on the rheological properties of the developed nanobubbles.

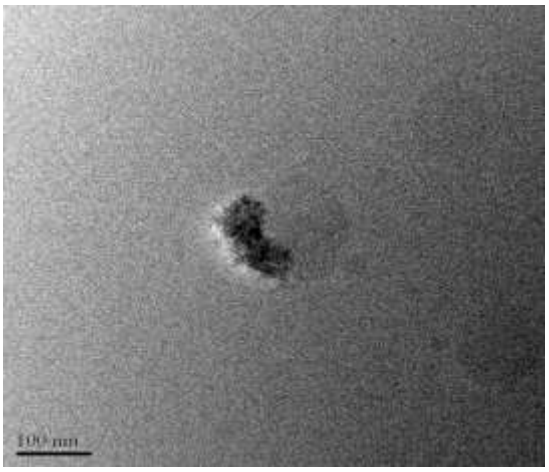

Figure 12. TEM image of ibrutinib nanobubbles

The DSC thermograms of pure ibrutinib, chitosan, blank nanobubbles, and ibrutinib-loaded chitosan nanobubbles are presented in **Figure 13**. The DSC thermogram of pure ibrutinib exhibited a sharp endothermic peak at **159.12°C**, corresponding to its melting point, confirming the crystalline nature of the drug. The DSC curve of chitosan showed a characteristic endothermic peak at **87.82°C**, which may be attributed to the loss of bound water present within the polymeric structure.

The DSC thermogram of blank chitosan nanobubbles exhibited two endothermic peaks. The first broad endothermic peak observed at approximately **73.40°C** was associated with the evaporation of residual water, whereas the second peak appearing in the temperature range of **90–100°C** was related to the thermal transition of the water-associated chitosan polymer matrix.

The chitosan nanobubble formulation demonstrated an endothermic peak at **98.34°C**, which showed a shift compared with the characteristic peak of pure chitosan (**87.82°C**). This shift in thermal transition temperature indicates structural modification and interaction within the polysaccharide matrix during nanobubble formation. Moreover, the disappearance of the characteristic melting endothermic peak of ibrutinib in the optimized nanobubble formulation suggests successful encapsulation and incorporation of the drug within the nanobubble core, confirming the molecular interaction between the drug and carrier system.

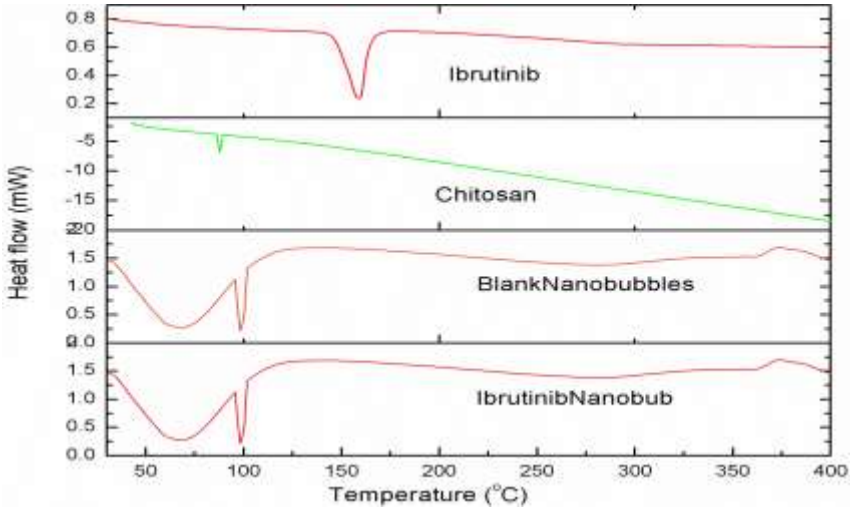

Figure 13. DSC thermogram of ibrutinib, Chitosan, blank nanobubbles and ibrutinib loaded nanobubbles

The in vitro release profile of ibrutinib from the nanobubble formulation was evaluated in the presence and absence of ultrasound stimulation and compared with the release behavior of ibrutinib suspension (**Figure 14**). The amount of drug released from the nanobubble formulation was significantly higher than that observed from the ibrutinib suspension, indicating the potential of nanobubbles as an effective drug delivery system.

A significant difference was observed between ultrasound-assisted and non-ultrasound-assisted drug release profiles. After 6 hours of incubation, the ultrasound-treated nanobubble formulation exhibited **48.53%** drug release, whereas only **18.88%** of ibrutinib was released from the formulation without ultrasound exposure. Furthermore, after 24 hours, the cumulative drug release from non-sonicated nanobubbles reached **54.76%**, while ultrasound exposure resulted in a significantly enhanced release of approximately **93.52%** of ibrutinib.

The enhanced drug release following ultrasound application may be attributed to the cavitation effect generated by ultrasound waves, which induces disruption of the nanobubble structure and promotes rapid release of the encapsulated drug. These findings demonstrate that ultrasound-triggered nanobubbles can provide controlled and site-specific delivery of ibrutinib with improved release efficiency.

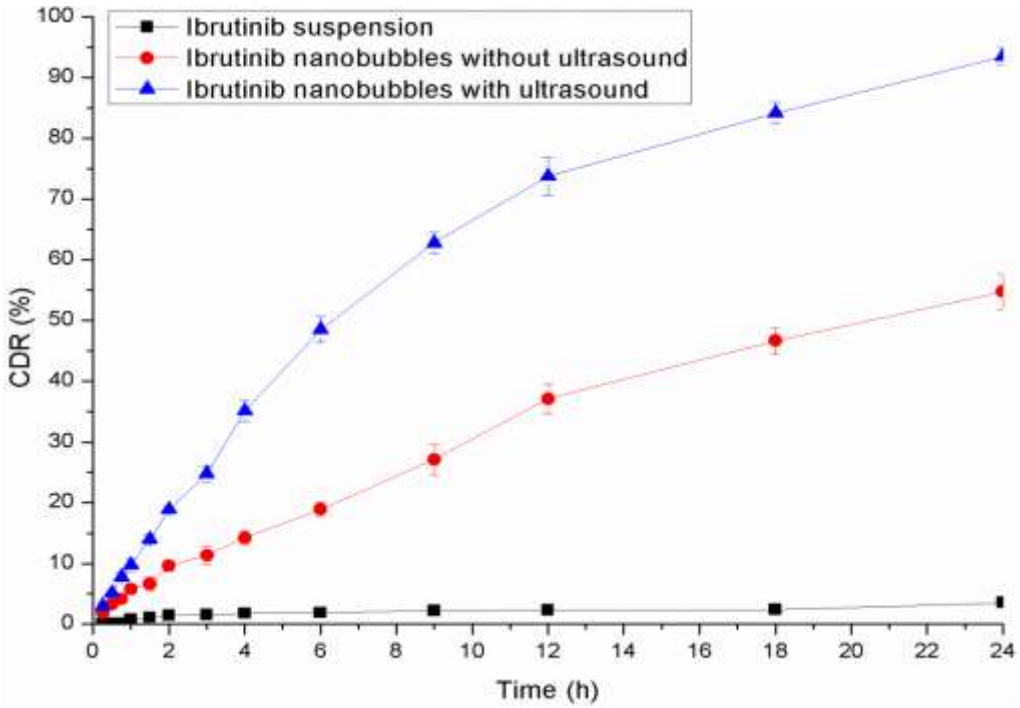

Figure 14. In-vitro drug release pattern with and without ultrasound assistance

The stability of ibrutinib-loaded nanobubbles following ultrasound exposure was evaluated at different temperatures to investigate the effect of sonication on nanobubble integrity. After 5 minutes of ultrasound treatment (2.5 MHz) at **25°C**, no significant changes were observed in the morphology and structural integrity of the nanobubbles, indicating good stability under these conditions. However, when ultrasound exposure was performed at **37°C**, gradual disruption of the nanobubble structure was observed. The nanobubbles started to disappear after 3 minutes of sonication and were completely

disrupted after 5 minutes of ultrasound exposure, suggesting reduced structural stability at physiological temperature due to ultrasound-induced cavitation effects.

The storage stability of the optimized ibrutinib-loaded nanobubble formulation was evaluated at different storage temperatures (**4°C, 25°C, and 40°C**) for a period of one month. The changes in drug content, encapsulation efficiency, and particle size at predetermined time intervals (**0, 15, and 30 days**) are presented in **Table 6**.

No significant changes in drug content were observed during storage at lower temperatures. The encapsulation efficiency remained almost unchanged at **4°C and 25°C**, indicating that the nanobubble system effectively protected ibrutinib from degradation and maintained formulation stability under normal storage conditions. In contrast, storage at elevated temperature (**40°C**) resulted in a significant reduction in encapsulation efficiency, which may be attributed to disruption of the nanobubble structure and leakage of the encapsulated drug. These findings suggest that the optimized nanobubble formulation possesses satisfactory stability when stored at refrigerated and ambient temperatures.

Table 6: Encapsulation efficiency, PLS and PI of ibrutinib nanobubbles stored at different temperatures

Temperature (°C)	Time (days)	Encapsulation efficiency(%)	PLS(nm)	PI
4 ±1 °C	0	82.58±3.17	201.66±7.12	0.16±0.005
	15	81.44±2.12	198.22±4.88	0.16±0.005
	30	81.12±0.96	197.33±3.94	0.17±0.005
25±2 °C	0	82.58±3.17	201.66±7.12	0.16 ± 0.005
	15	80.12±1.76	196.22±4.88	0.182±0.005
	30	79.88±1.92	195.33±3.94	0.224±0.005
40±2 °C	0	82.58±3.17	201.66±7.12	0.16 ± 0.005
	15	77.72±0.88	248.12±1.84	0.236±0.005
	30	72.12±2.06	376.34±2.12	0.388±0.005

n = 3 ($p < 0.05$)

The evaluation of hemocompatibility is an essential requirement for formulations intended for parenteral administration. Therefore, the hemolytic activity of blank chitosan nanobubbles and ibrutinib-loaded chitosan nanobubbles was investigated to assess their safety profile. The aqueous suspension of chitosan nanobubbles exhibited no significant hemolytic activity up to the tested concentration of **5 mg/mL**, indicating good blood compatibility of the carrier system. Similarly, ibrutinib-loaded nanobubbles demonstrated a favorable safety profile with erythrocytes, suggesting that incorporation of the drug did not adversely affect the hemocompatibility of the formulation.

In Vitro Cellular Uptake Study

The cellular uptake efficiency of ibrutinib from the nanobubble formulation was evaluated in HepG2 cells by measuring fluorescence intensity (**Figure 15**). After 2 hours of incubation, the fluorescence intensity of treated cells was analyzed to compare the uptake of free and ultrasound-treated formulations.

HepG2 cells treated with ultrasound-assisted ibrutinib-loaded nanobubbles exhibited a mean fluorescence intensity of **6.12**, which was approximately **1.5-fold higher** than that observed in cells treated with ibrutinib-loaded nanobubbles without ultrasound exposure. The enhanced fluorescence intensity following ultrasound treatment indicates improved cellular internalization of ibrutinib from the nanobubble system. This increased uptake may be attributed to ultrasound-induced cavitation effects, which enhance membrane permeability and facilitate the intracellular delivery of the encapsulated drug.

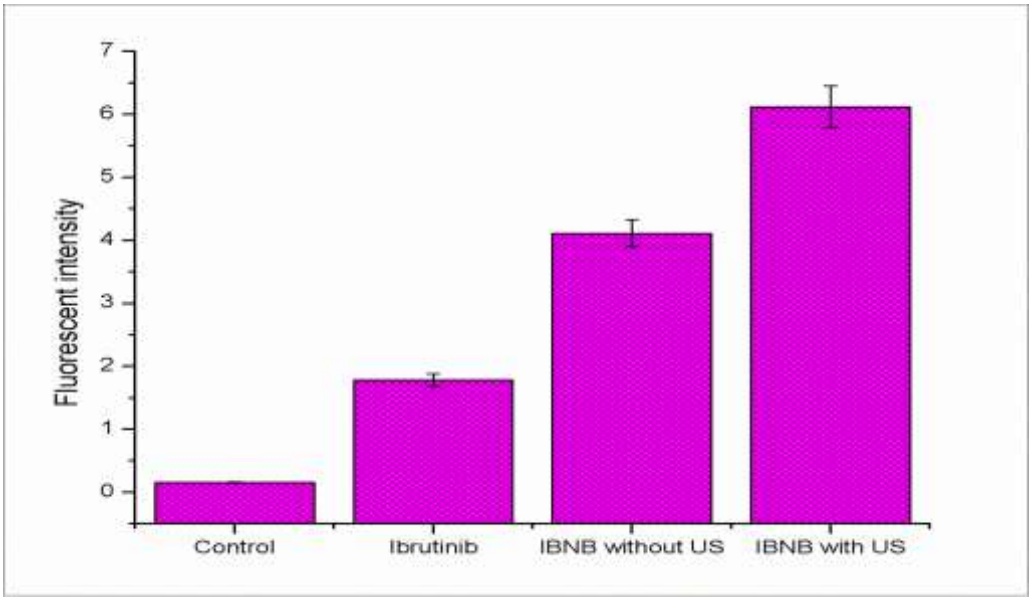

Figure 15: Results of Cellular uptake study

In Vitro Cytotoxicity Study

The in vitro cytotoxic activity of free ibrutinib and ibrutinib-loaded nanobubble formulations against HepG2 cells was evaluated using the MTT assay (**Figure 16**). HepG2 cells exhibited more than **98% cell viability** when treated with different formulations at a lower drug concentration of **10 µM**, indicating minimal cytotoxicity at this concentration.

Similarly, cell viability remained above **83%** even at an ibrutinib concentration of **20 µM**, which may be attributed to the concentration being below the effective cytotoxic dose required to induce significant cell death. However, a concentration-dependent reduction in cell viability was observed with increasing drug concentration for all tested formulations.

Among the evaluated formulations, ultrasound-assisted ibrutinib-loaded nanobubbles demonstrated the highest cytotoxic effect, resulting in the lowest cell viability compared with free ibrutinib and non-sonicated ibrutinib-loaded nanobubbles. The calculated IC_{50} values for free ibrutinib, ibrutinib-loaded nanobubbles without ultrasound, and ultrasound-assisted ibrutinib-loaded nanobubbles were found to be **94.2, 81.76, and 70.42 µM**, respectively.

The reduced IC_{50} value of ultrasound-assisted nanobubbles indicates enhanced anticancer activity, which may be attributed to ultrasound-triggered drug release, improved cellular uptake, and increased intracellular availability of ibrutinib. These findings suggest that ultrasound-responsive nanobubbles can improve the therapeutic efficacy of ibrutinib by facilitating efficient drug delivery to cancer cells.

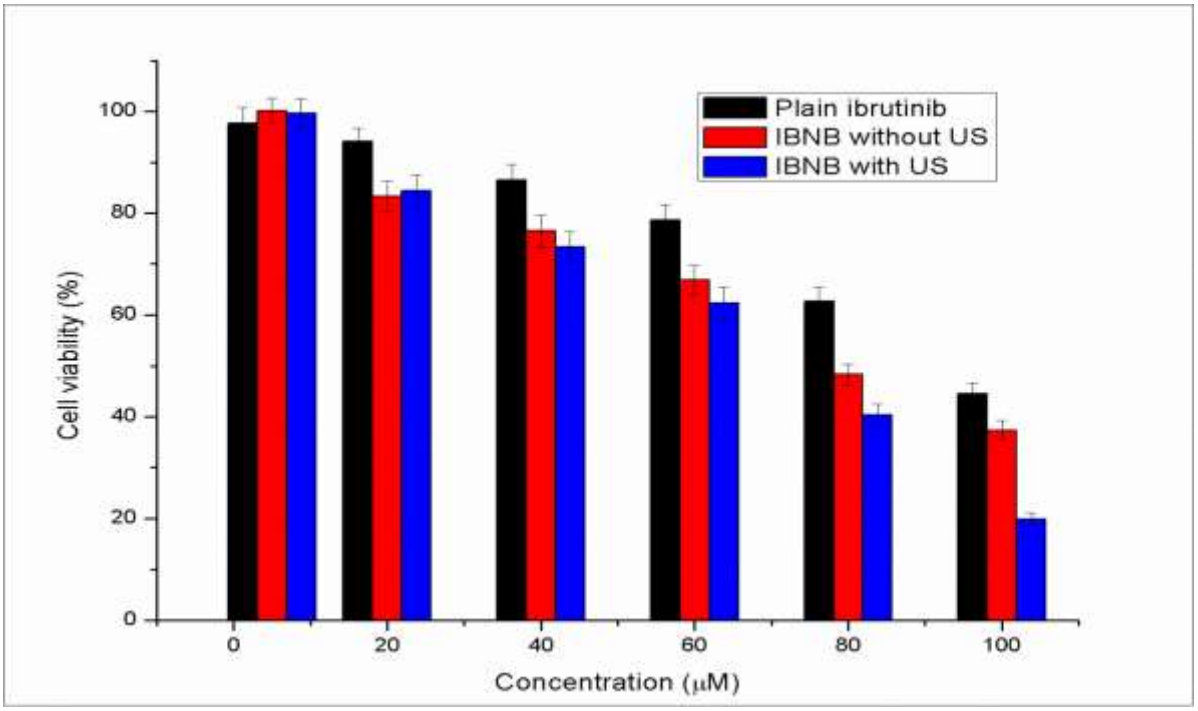

Figure 16: In vitro cytotoxicity of plain ibrutinib, ibrutinib nanobubbles without ultrasound and ibrutinib nanobubbles with ultrasound

Conclusion

In the present study, chitosan-shelled and perfluoropentane-core nanobubbles were successfully developed as a novel delivery system for the anticancer drug ibrutinib. The formulation variables were systematically optimized using response surface methodology to obtain nanobubbles with desirable particle size and size distribution characteristics. The optimized nanobubble formulation exhibited uniform particle size distribution and improved physicochemical properties.

Compared with the conventional ibrutinib suspension, the developed nanobubble formulation demonstrated enhanced drug solubility under different pH conditions. The in vitro drug release study revealed improved dissolution behavior and ultrasound-responsive release characteristics of ibrutinib-loaded nanobubbles. Furthermore, the formulation exhibited good stability and enhanced anticancer activity, as demonstrated by in vitro cytotoxicity studies, showing improved inhibition of tumor cell growth compared with free drug treatment.

Overall, the findings of this study suggest that chitosan-based nanobubbles represent a promising and efficient drug delivery platform for improving the therapeutic performance of ibrutinib.

References

1. Peer D, Karp JM, Hong S, Farokhzad OC, Margalit R, Langer R. Nanocarriers as an emerging platform for cancer therapy. *Nature Nanotechnology*. 2007;2:751-760.
2. Blanco E, Shen H, Ferrari M. Principles of nanoparticle design for overcoming biological barriers to drug delivery. *Nature Biotechnology*. 2015;33:941-951.
3. Torchilin VP. Multifunctional nanocarriers. *Advanced Drug Delivery Reviews*. 2012;64:302-315.

4. Kooiman K, Roovers S, Langeveld SAG, Kleven RT, Dewitte H, Ogris M, et al. Ultrasound-responsive nanobubbles for drug and gene delivery. *Advanced Drug Delivery Reviews*. 2014;72:28-48.
5. Chen LE, Nittayacharn P, Exner AA. Progress and potential of nanobubbles for ultrasound-mediated drug delivery. *Expert Opinion on Drug Delivery*. 2025;22(7):1007-1030.
6. Cavalli R, Bisazza A, Trotta M, Argenziano M, Civra A, Donalisio M, Lembo D. New chitosan nanobubbles for ultrasound-mediated gene delivery: preparation and in vitro characterization. *International Journal of Nanomedicine*. 2012;7:3309-3318.
7. Agnihotri SA, Mallikarjuna NN, Aminabhavi TM. Recent advances on chitosan-based micro- and nanoparticles in drug delivery. *Journal of Controlled Release*. 2004;100:5-28.
8. Bernkop-Schnürch A, Dünnhaupt S. Chitosan-based drug delivery systems. *European Journal of Pharmaceutics and Biopharmaceutics*. 2012;81:463-469.
9. Dash M, Chiellini F, Ottenbrite RM, Chiellini E. Chitosan—A versatile semi-synthetic polymer in biomedical applications. *Progress in Polymer Science*. 2011;36:981-1014.
10. Abdullah S, Mohammad J, Anwer A, Majid A. Enhanced oral bioavailability of ibrutinib encapsulated polymeric nanoparticles: pharmacokinetic evaluation in rats. *Current Pharmaceutical Analysis*. 2019;15:661-668.
11. Zhang S, Li J, Lyu Y, et al. Nanotechnology-based strategies for improving the delivery and therapeutic efficacy of anticancer drugs. *International Journal of Nanomedicine*. 2021;16:6655-6678.
12. Waller CF. Ibrutinib in the treatment of B-cell malignancies. *Clinical Advances in Hematology & Oncology*. 2016;14:23-31.
13. Byrd JC, Furman RR, Coutre SE, et al. Targeting BTK with ibrutinib in B-cell malignancies. *New England Journal of Medicine*. 2013;369:32-42.
14. Gajra B, Dalwadi C, Patel R. Formulation and optimization of polymeric lipid hybrid nanoparticles using Box–Behnken design. *Journal of Pharmaceutical Innovation*. 2015;10:1-12.
15. Li W, Zhang X, Jing S, Xin X, Chen K, Chen D, Hu H. Preparation and optimization of nanoparticles using Box–Behnken design for drug delivery applications. *Journal of Pharmaceutical Sciences*. 2017;106:2053-2059.
16. Shaikh MV, Kala M, Nivsarkar M. Formulation and optimization of anticancer drug-loaded polymeric nanoparticles using Box–Behnken design: in vitro and in vivo evaluation. *European Journal of Pharmaceutical Sciences*. 2017;101:51-62.